



ARTICLE

## A Design of Predictive Intelligent Networks for the Analysis of Fractional Model of TB-Virus

Muhammad Asif Zahoor Raja<sup>1</sup>, Aqsa Zafar Abbasi<sup>2</sup>, Kottakkaran Sooppy Nisar<sup>3,\*</sup>, Ayesha Rafiq<sup>2</sup> and Muhammad Shoaib<sup>4</sup>

<sup>1</sup>Future Technology Research Center, National Yunlin University of Science and Technology, 123 University Road, Section 3, Douliou, Yunlin, 64002, Taiwan

<sup>2</sup>Department of Applied Mathematics and Statistics, Institute of Space Technology, Islamabad, 44000, Pakistan

<sup>3</sup>Department of Mathematics, College of Science and Humanities in Al-Kharj, Prince Sattam bin Abdulaziz University, Al-Kharj, 11942, Saudi Arabia

<sup>4</sup>AI Center, Yuan Ze University, Taoyuan, 320, Taiwan

\*Corresponding Author: Kottakkaran Sooppy Nisar. Email: n.sooppy@psau.edu.sa

Received: 02 September 2024; Accepted: 19 March 2025; Published: 30 May 2025

**ABSTRACT:** Being a nonlinear operator, fractional derivatives can affect the enforcement of existence at any given time. As a result, the memory effect has an impact on all nonlinear processes modeled by fractional order differential equations (FODEs). The goal of this study is to increase the fractional model of the TB virus's (FMTBV) accuracy. Stochastic solvers have never been used to solve FMTBV previously. The Bayesian regularized artificial (BRA) method and neural networks (NNs), often referred to as BRA-NNs, were used to solve the FMTBV model. Each scenario features five occurrences that each reflect a different order of derivatives, ranging from 0.8, 0.85, 0.9, 0.95, and 1, as well as five potential rates for different parameters. Training data made up 90% of the data, testing data made up 5%, and validation data made up 5% of the data used to illustrate the FMTBV's approximations. To verify that the BRA-NNs were correct, the generated simulations were described in the following solutions using the FOLotkaVolterra approach in MATLAB. Comprehensive Simulink results in terms of mean square error, error histogram, and regression analysis investigations further highlight the competence, dependability, and accuracy of the suggested BRA-NNs.

**KEYWORDS:** Fractional model of TB-Virus (FMTBV); artificial neural network; bayesian regularization

### 1 Introduction

"*Mycobacterium tuberculosis*" is the bacterium that causes "tuberculosis" (TB). Although the lungs are usually affected, other organs like the spine, brain, as well as kidneys may also be affected. Droplets containing germs are released into the air and consumed by others when an infected person coughs, sneezes, or talks. The bacteria-containing particles are inhaled by others when an infected person coughs, sneezes or speaks. Once within the body, tuberculosis can spread and lead to an infection. On the other hand, not all TB patients experience active illnesses. A persistent TB infection is typically the result of the immune system suppressing the illness [1]. Congenital tuberculosis patients are asymptomatic and not contagious, but if their immune systems are weakened, the bacteria may stay dormant in their organs and later emerge active. Worldwide TB Burden: By 2020, the World Health Organization (WHO) predicts that 10 million people will get TB globally. The number of TB-related deaths: According to [2], TB claimed the lives of almost 1.5 million people in 2020. People who are actively TB-positive exhibit clinical TB symptoms and run the risk of spreading



the illness to others. People who have active tuberculosis may cough up blood or sputum, have a phlegm-producing cough, chest pain, exhaustion, loss of weight, night sweats, and appetite loss. Usually, symptoms get worse with time, but they can also go away on their own and come back. One of the most important methods for characterizing and comprehending systems of various degrees that result from interactions is mathematical modelling [3]. Many mathematical models were created and examined over time to explain the dynamics of tuberculosis epidemiology in the general population. A computational framework was developed in [4] to investigate the dynamics of tuberculosis transmission that takes exogenous re-infection into account. It was demonstrated that the inclusion of exogenous recurrence in the model significantly alters the disease's qualitative dynamics, increasing the likelihood of several chronic points of equilibrium at the crucial basic reproduction number threshold. Huo et al. [5] developed and examined an unpredictable mathematical model that took into account both hospital and home therapy for TB infectious persons. It was found that home treatment significantly impacted the dynamics of TB transmission. Few research has taken into account the fractional derivative operator while simulating the dynamics of TB epidemiology. Notably, the authors in [6] investigated the issue of optimal control for the fractional-order TB infection model combining diabetic and resistant strains using the Atangana–Baleanu–Caputo (ABC) derivative operator. A discrete fractional framework for tuberculosis in the form of the Caputo derivative was proposed by Altaf Khan et al. [7], who also looked into how the model parameters affected the system's behavior. A TB model with continuous control measures using the Caputo fractional operator was examined by Owolabi et al. [8]. The scientists concluded that a model that included a fractional order component could provide a good control measure against the spread of tuberculosis in the population after conducting some numerical tests. Using the Laguerre polynomial, the authors in [9] applied fractional-order derivatives of Caputo type to the dynamics of TB transmission. The authors concluded that fractional-order derivatives are more capable of handling real-world scenarios than the typical classical-order models. Ullah et al. [10] analyzed a five-dimensional mathematical model that described the transmission dynamics of tuberculosis in the human population using non-integer-order derivatives of Caputo sense. In a related advancement, Farman et al. [11] used non-integer-order differential equations to create a six-dimensional system of differential equations to investigate how treatment affects the dynamics of tuberculosis transmission. In [12], the authors have done the mathematical analysis of a fractional operator-based TB model. To describe the changing patterns of TB infection *in vivo*, this work presents a unique model that takes host cell encounters with *Mycobacterium tuberculosis* into consideration. In addition to the TB virus, fractional derivatives have recently been used to study the dynamics of a recently created co-infection model of the HIV and HCV [13] as well as the dynamic behaviors of the HBV under the influence of cytokines and immune response [14].

An empirical concept called an Artificial Neural Network (ANN) aims to replicate the structure and relationships between neurons in the brain. The basic mathematical model (function) of an ANN begins with an input neuron. Three basic rules: amplification, gathering, and activation—control this model. At the time of termination of an artificial neuron, the sum of the previous weights for connections and selectivity passes through an activation function, also known as a transfer function. When ANNs are connected, their full potential and decoding capability become apparent, even though their physics and basic set of rules may not seem very remarkable. These ANNs are predicated on the idea that variation might result from a few straightforward concepts. Instead of just making the system complex and unmanageable, we often don't link these artificial neurons carelessly to exactly benefit from the computational demands that may be met by connecting numerous ANs. Several “highly standardised” surface properties for ANNs have previously been produced by researchers. Problem solving may be facilitated by these preset traits, which have the potential to be even more successful. Various problems can be solved more successfully with different ANN topographies. Determine the type of problem that has to be solved before selecting and properly implementing the ANN's design. It is necessary to modify the architecture and its components. The ANN is a necessary component of

every ANN. Its form and function were modelled after the genuine neuron, which is thought to be the basic building component of biological NNs (operations) such as the cerebral cortex, brain stem, and surrounding glands. Recently, ANN approach has been applied to investigate the plant virus [15] and the Stuxnet virus [16].

**a) Objective:**

All of the above amazing uses encourage authors to explore the machine learning paradigm by developing a Bayesian regularization approach for fractional models of the TB virus (FMTBV) based on neural network (BRA-NNs). The developed determining BRA-NNs plan has the following aims in the future:

- The findings obtained using the BRA-NNs approach are compared to the exact solutions for six different FMTBV variants.
- Five suitable fractional-order versions based on the numerical solution of the FMTBV mathematical model, demonstrating the reliability of the BRA-NNs.
- The outcomes of the FOlotkaVolterra technique’s produced and referenced solutions are compared, and it is shown that they are extremely congruent, proving the correctness of the randomized computationally integrator based on BRA-NNs.
- The performance of the created BRA-NNs system is assessed using in-depth study on the error histogram, Mean Square Error, regression analysis and transition statistics measures.

**b) Layout:**

The study is arranged in the form that an orderly and step-by-step introduction of concepts and methods used closely follows after the results and conclusions. Section 2, first of all, a general fundamental overview is needed regarding some definitions of fractional derivatives, which are now considered to be necessary when the modelization of complex dynamic systems requires it, followed then by the introduction of TB virus fractional model, that mathematically frames the subject of the study. The discretization techniques used in the analysis are further explained in Section 3, where the Grünwald-Letnikov scheme for the discretization of fractional derivatives and BRA-NN, how to solve and analyze the model, are also presented. Section 4 states the results and the analysis of the simulation. Finally, Section 5 summarizes key findings and implications of further work that may be achieved for modeling fractional systems such as the TB virus, based on the possible impact of BRA-NN and GL methods.

**2 Preliminaries and Mathematical Model**

In this section, firstly, we will discuss some basics regarding fractional integral and Caputo fractional order derivative. After we will discuss the methodology that is Bayesian regularization.

**a) Basic Definitions:**

**Definition 1:** For a function  $g: \mathbb{R}^+ \rightarrow \mathbb{R}$ , the fractional integral of order  $\tilde{\alpha} > 0$  is defined by

$$I_t^{\tilde{\alpha}}(g(t)) = \frac{1}{\Gamma(\tilde{\alpha})} \int_0^t (t - \dot{X})^{\tilde{\alpha}-1} g(\dot{X}) d\dot{X}$$

The Gamma function is denoted by  $\Gamma$  here and elsewhere.

**Definition 2:** The following gives the Caputo fractional order derivative for the function  $g \in C^n$  of order  $\tilde{\alpha}$ :

$${}_c D_t^{\tilde{\alpha}}(g(t)) = I^{n-\tilde{\alpha}} D^n g(t) = \frac{1}{\Gamma(n - \tilde{\alpha})} \int_0^t \frac{g^n(\dot{X})}{(t - \dot{X})^{\tilde{\alpha}+n-1}} d\dot{X}$$

This is clearly defined for functions that are absolutely continuous and  $n - 1 < \tilde{\alpha} < n \in \mathbb{N}$ . Note that all values of  $g(n)$ , for  $\tilde{X} \in [0, t]$ , are included in the value of the Caputo fractional derivative of the function  $g$  at point  $t$ . It is obvious that  ${}_t^c \mathcal{D}_t^{\tilde{\alpha}} (g(t))$  tends to  $g(t)$  as  $\tilde{\alpha} \rightarrow 1$ .

**Definition 3:** The constant  $z^*$  is the system's equilibrium point in the below-mentioned Caputo fractional dynamical system.

$${}_t^c \mathcal{D}_t^{\tilde{\alpha}} z(t) = f(t, z(t)), \tilde{\alpha} \in (1, 0)$$

only if and when,  $f(t, z^*) = 0$ .

**b) Mathematical Model:**

We offer the proposed fractional model to explain the dynamics of TB infection (FMTBV) in this section. The whole human population is separated into five epidemiological sub-divisions to develop the model: susceptible  $\mathcal{S}(t)$ , exposed  $L(t)$ , TB active  $I(t)$ , under treatment  $\check{T}(t)$ , and recovered persons after treatment  $\mathcal{R}(t)$ .

The system of non-linear fractional differential equations that follows provides the transmission model for TB dynamics:

$$\begin{aligned} {}_t^c \mathcal{D}_t^{\tilde{\alpha}} \mathcal{S} &= \Lambda - \frac{\beta \mathcal{S} I}{\tilde{N}} - \hat{u} \mathcal{S} \\ {}_t^c \mathcal{D}_t^{\tilde{\alpha}} L &= \frac{\beta \mathcal{S} I}{\tilde{N}} - (\hat{u} + \varepsilon) L + (1 - n) \sigma \check{T} \\ {}_t^c \mathcal{D}_t^{\tilde{\alpha}} I &= \varepsilon L + n \sigma \check{T} - (\hat{u} + \gamma + \sigma_1) I \\ {}_t^c \mathcal{D}_t^{\tilde{\alpha}} \check{T} &= \gamma I - (\hat{u} + \sigma + \sigma_2 + \xi) \check{T} \\ {}_t^c \mathcal{D}_t^{\tilde{\alpha}} \mathcal{R} &= \xi \check{T} - \hat{u} \mathcal{R} \end{aligned}$$

The starting circumstances are

$$\mathcal{S}(0) = \mathcal{S}_0, L(0) = L_0, I(0) = I_0, \check{T}(0) = \check{T}_0, \text{ and } \mathcal{R}(0) = \mathcal{R}_0.$$

The parameter  $\tilde{\alpha} \in [0, 1]$  and the fractional derivatives used in the aforementioned model are both taken in Caputo meaning. All of the functions  $\mathcal{S}$ ,  $L$ ,  $I$ ,  $\check{T}$ , and  $\mathcal{R}$ , together with their Caputo fractional derivatives, are considered to be continuous for all  $t \geq 0$ . Table 1 provides a detailed overview of the model parameters and their fitted or estimated numerical values.

**Table 1:** Parameter's description

Symbol	Description	Symbol	Description
$\Lambda$	Recruitment rate	$\beta$	Transmission rate
$\sigma_2$	Disease induced death rate in T	$\hat{u}$	Natural death rate
$\varepsilon$	Rate of progression from L to I	$n$	Rate of treatment failure
$\xi$	Moving rate from T to R	$\sigma$	Rate at which treated people leave T class
$\gamma$	progression rate from I to T	$\sigma_1$	Disease induced death rate of infected individuals

### 3 Methodology

#### 3.1 Fractional Differential Equation's Stochastic Analyzer Based on Grunwald-Letnikov

The Grünwald-Letnikov (G-L) approach is regularly applied, but the total of the strategy lengthens over time, highlighting the flaw. The factors  $c_v$  are thorough approaches with properties that improve service, such as being favorable and having a significant attenuation effect. They conclude that the approach offers seamless features although the corrective term causes some disturbance. A discrete version of the Gronwall defense is very helpful in demonstrations. The G-L approximation is used as a numerical tool to study robustness and incorrect predictions related to linear test equations.

Consider generic version of an FDE and its initial circumstances to illustrate the numerical results for FDEs relying on G-L:

$$\begin{aligned} {}_a^c D_t^\beta &= f(r, s(t)), \\ s^{(i)}(0) &= s_0^{(i)}, i = 0, 1, \dots, n-1 \end{aligned} \tag{1}$$

Ivo Petras provided a detailed final cyclical prescription of a GL-based solution obtained from Eq. (1):

$$\frac{1}{h^\beta} \sum_{o=0}^{[(r-a)*1/h]} (-1)^o s(r-oh) \binom{\beta}{o} \approx f(s(t) t) \tag{2}$$

To summarize the aforementioned relationship, we obtain

$$\sum_{o=0}^{[(r-a)*1/h]} (-1)^o s(r-oh) \binom{\beta}{o} + r(t) \approx h^{-\beta} f(r, s(t)) \tag{3}$$

In the form of nonlinear input grid systems, the interval  $t \in [0, T] = [0, h, 2h, \dots, Kh = T]$ , where  $h$  is the step size indicator,  $[0, T] = t_0 = 0, t_1, \dots, t_K = T$ , as well as any system to collect in the interval were also depicted as  $t_k = kh$  for  $k = 0, 1, 2, \dots, K$ . The aforementioned equation is represented as follows in discrete form:

$$\sum_{o=1}^k (-1)^o \binom{\beta}{o} s(r_k - oh) + s(r_k) = h^{-\beta} f(r_k, s(r_k)), k = 0, 1, 2, \dots, K$$

In simple usage, the above term is written as:

$$\sum_{o=1}^k c_o^\beta y(t_k - ho) + y(r_k) = h^{-\beta} f(r_k, s(r_k)), k = 0, 1, 2, \dots, K$$

where  $c_o^\beta$  is defined as:

$$c_o^\beta = \binom{\beta}{o} (-1)^o$$

or equivalently with  $c_o^\beta = 1$ ,

$$c_o^\beta = \left(1 - \frac{1+\beta}{o}\right) c_{o-1}^\beta, o = 0, 1, \dots$$

The recursive form of the GL numerical solver is:

$$s(r_k) = - \sum_{o=1}^k c_o^\beta y(r_{k-o}) + h^{-\beta} f(r_k, s(r_k)), k = 0, 1, 2, \dots, k$$

### 3.2 Proposed Methodology

As a suitable analogue to such a speculative neural network, we propose a Bayesian regularized artificial neural network (BRA-NNs) with particular properties that relate readily to physiochemical features. The use of BRA-NNs has the benefit of strong predictions without the need for the recognition technique, which in traditional regression algorithms rises as  $O(N^2)$ . Strength training is difficult since it does not require specific validation data to indicate overtraining and instead gives the ideal point at which to cease training. The BRA-NN network architecture is essentially unimportant as long as a minimum design is offered. To properly define the words Bayesian and regularized, basic regression procedures must be presented in Bayesian terms. Because terminology and depictions differ from approach to approach, generating issues, the included depictions are standard but occasionally strange. It is feasible to accomplish at an equilibrium level rather than the generally accepted least amount because the approach employs a gradient decreasing descent or an analogous lowest reported. Five times through this method is all that is necessary, according to observation, to end any unusual behavior. In contrast, embodied ANNs enable trials with hundreds or possibly thousands of repetitions. In addition to avoiding overfitting, it offers a more reliable estimation of the model coefficients. An overview of the Bayesian regularization algorithm is provided below:

1. **Initialize the variables:** Define the model coefficients' previous distribution.
2. **Data preparation:** Prepare your dataset, including the input features (X), goal values (Y), and any other relevant information.
3. **Feature standardization (optional):** Standardizing the input features to have a zero mean and unit variance is typically a good idea. Although this step is optional, it occasionally can be beneficial.
4. **Model training:** Apply Bayesian inference to estimate the model's parameters. the following steps:
  - **Prior Distribution:** Define the model coefficients' previous distribution. The prior is often assumed to be Gaussian with a variance parameter and a mean of zero in Bayesian ridge regression.
  - **Likelihood Function:** Establish the likelihood function, which, given the model and the input features, provides the likelihood of seeing the target values. The likelihood in linear regression is frequently taken to be Gaussian.
  - **Distribution in the rear:** Using Bayes' theorem, combine the prior distribution and likelihood function to get the posterior distribution of the model coefficients.
  - **Estimation of the parameter:** To estimate the model coefficients from the posterior distribution, use the appropriate technique (for instance, Maximum A Posteriori estimation or Markov Chain Monte Carlo methods).
5. **Model prediction:** Use the obtained model coefficients to create predictions about fresh data points.
6. **Model assessment (optional):** Use the proper metrics (e.g., mean squared error, mean absolute error, etc.) on a validation set or through cross-validation to assess the performance of the Bayesian regularized model.
7. **Tuning of hyperparameters (optional):** Hyperparameters that are part of the Bayesian regularization process, such as the variance parameter, can be tuned using methods like cross-validation to determine the best values that maximize the model's performance.
8. **Forecast based on new data:** You can use the model to generate predictions on fresh, unforeseen data after it has been trained and tweaked.

### 4 Results and Discussion

The FMTBV mathematical paradigm is discussed in this section utilizing the recommended BRA-NNs structure. The approach consists of two elements. First, the fundamental BRA-NNs controller discoveries are given. The BRA-NNs implementation approach is also used to resolve the FMTBV mathematical framework. Fig. 1 shows the single-layer layout of neurons. The “nftool” function in MATLAB provides access to the BRA-NNs processes, which use the following data configuration: 90% for training, 5% for testing, and 5% for authorization. Fig. 2 depicts the graphical presentation of the proposed scheme, i.e., BRA-NNs for FMTBV. Table A1 illustrates the simulations of BRA-NNs for FMTBV. Reference datasets are generated using FOLotkavoltera which is based on Grunwald Letnikov method. The data set for scenario I’s case I is presented in Table A2. Complete size of all data sets for each case is  $200 \times 5$  with step size 0.5.

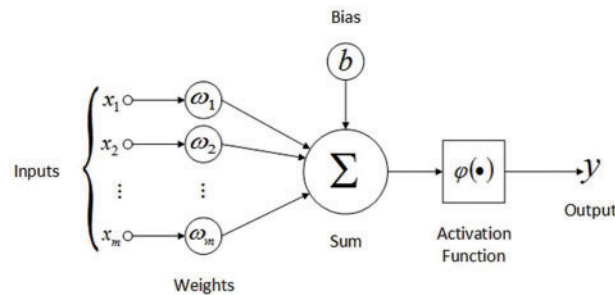


Figure 1: Single layer neuron formation

## ANALYSIS OF FRACTIONAL MODEL OF THE TB VIRUS USING ARTIFICIAL NEURAL NETWORK

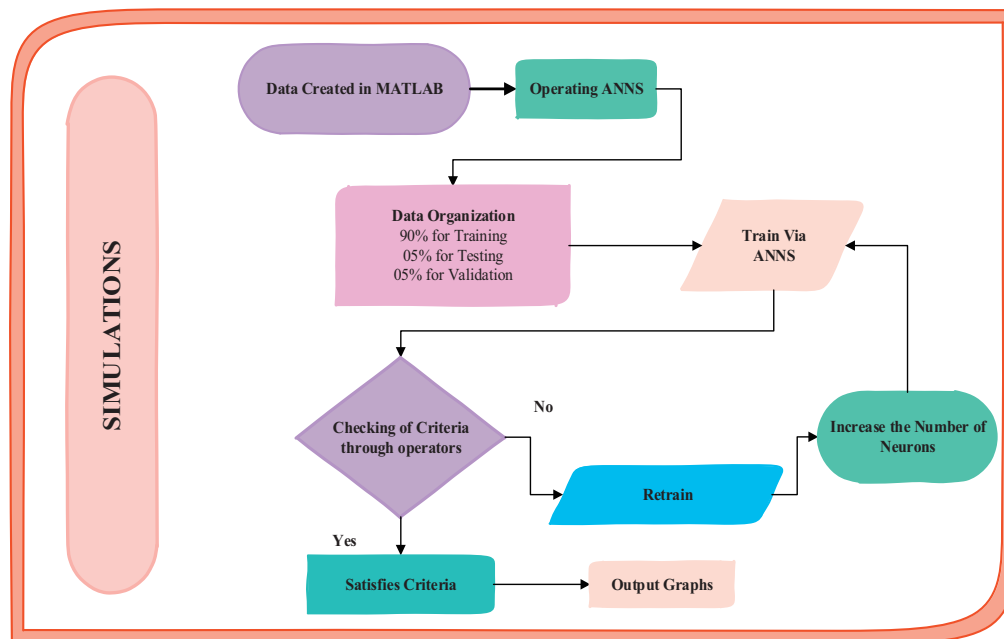
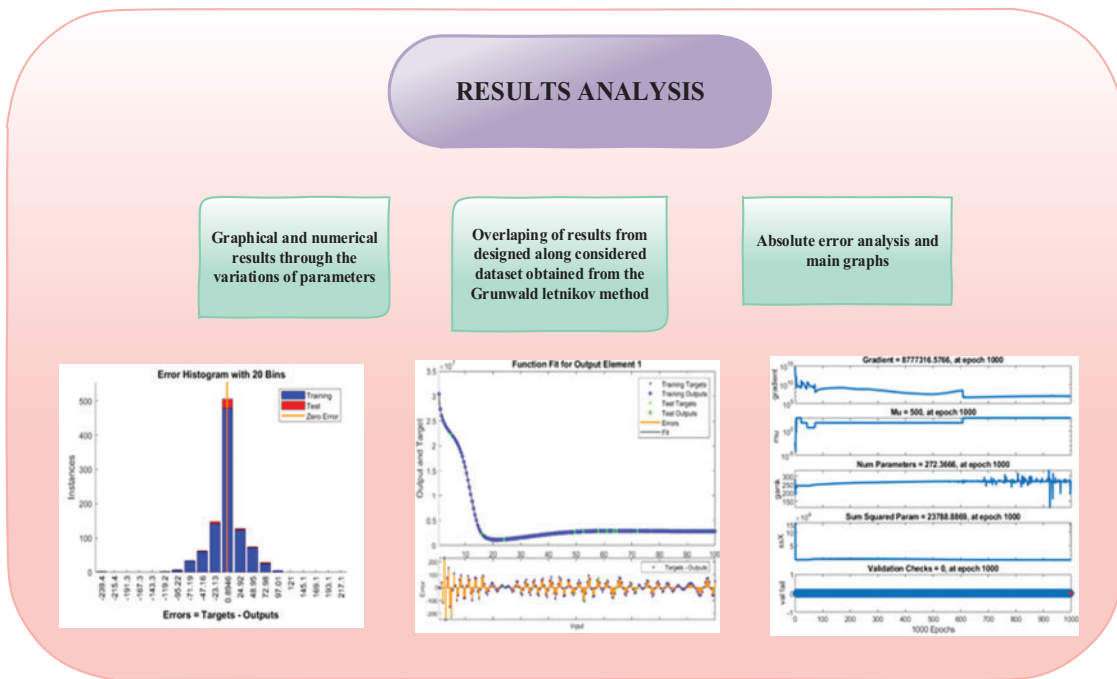


Figure 2: (Continued)



**Figure 2:** Graphical simulations of BRA-NNs for FMTBV

Figures relating to performance plot, i.e., mean squared error (MSE), transition state (TS), fitness curve (FC), error histogram (EH), and regression analysis (RA) are included in Figs. 3 and 4, which illustrate the BRA-NNs numerical simulation for FMTBV for scenarios I-Case III and II-Case III, respectively. In neural networks, the Mean Squared Error (MSE) loss function is frequently used to calculate the discrepancy between expected and actual output values. It measures the total discrepancy between the predicted values of the network and the exact target values. The neural network's training function is referred to as "trainFcn". The network's training performance and speed can be considerably impacted by the training function that is used. Regularization is a method for keeping neural networks from overfitting. It aids in striking a balance between the network's capacity (complexity) and adaptability to new inputs. Typically, a regularization parameter with a value between 0 and 1 is indicated. Overfitting may be avoided by using a larger regularization value, prioritizing minimizing squared biases and weights above reducing errors. A preprocessing method called normalization is used to scale data into a particular range. Normalization is used in the context of neural networks to affect the input data and target values. Normalization choices include "no," "standard," and "percent." For BRA-NNs, the transition state consists of five different components: the gradient, Mu, Num parameters, sum squared parameter, and validation check. The vector of a function's partial derivatives about its inputs is referred to as the gradient. The method of updating the model's parameters during training is employed in neural network optimization. As a hyper parameter used in optimization methods like gradient descent, Mu often refers to the learning rate. The step size used for parameter updates is determined by the learning rate. The number of learnable weights and biases is represented by the num-parameter in the context of neural networks. In machine learning, the term "sum squared parameter" is not commonly used. Without more information, it's difficult to give a precise explanation, however, it might be a reference to a certain formula or technique. The process of assessing a trained model's performance using a different dataset known as the validation set is known as the validation check.

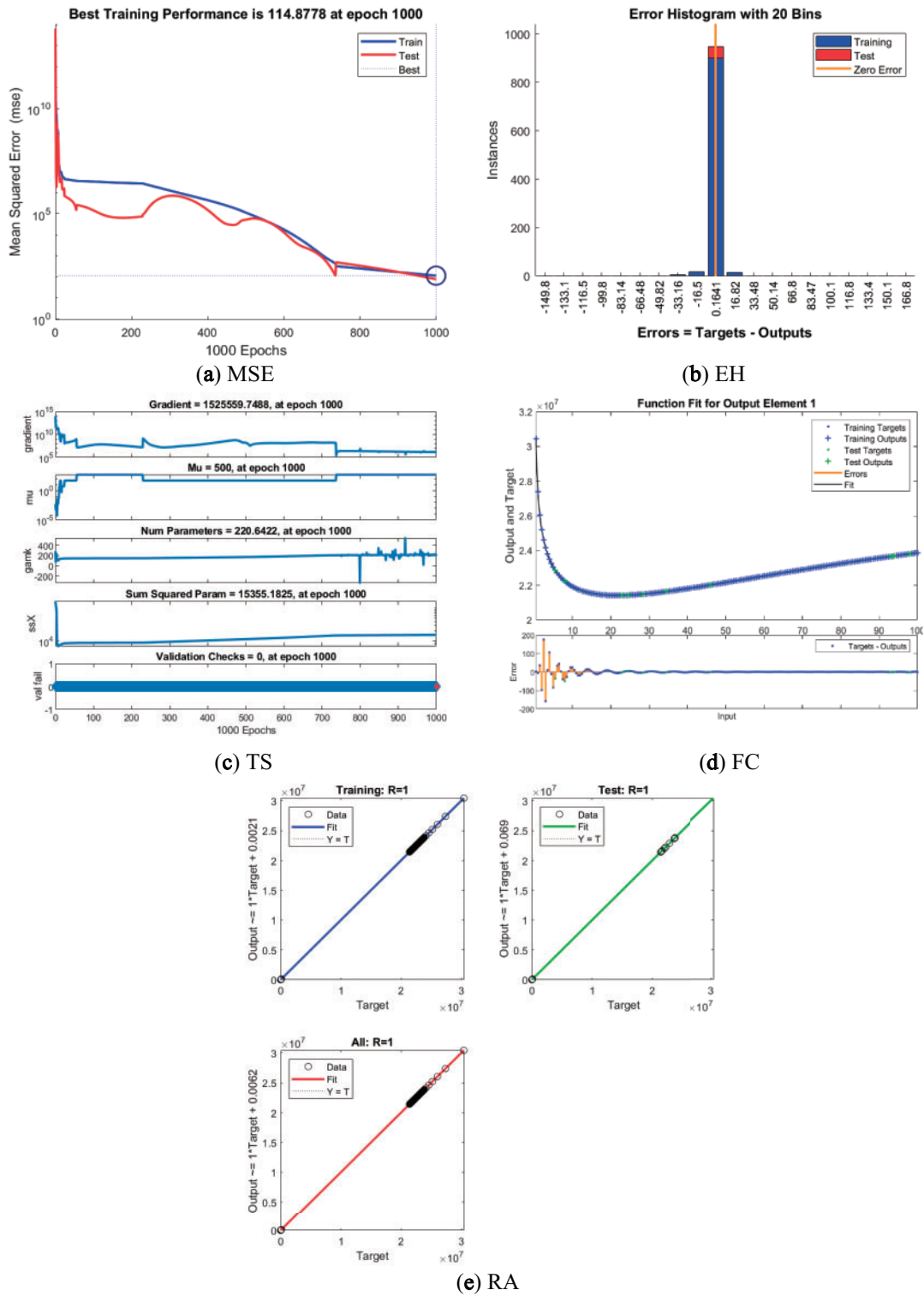


Figure 3: Graphical outputs based on BRA-NNs for scenario 1 case 3

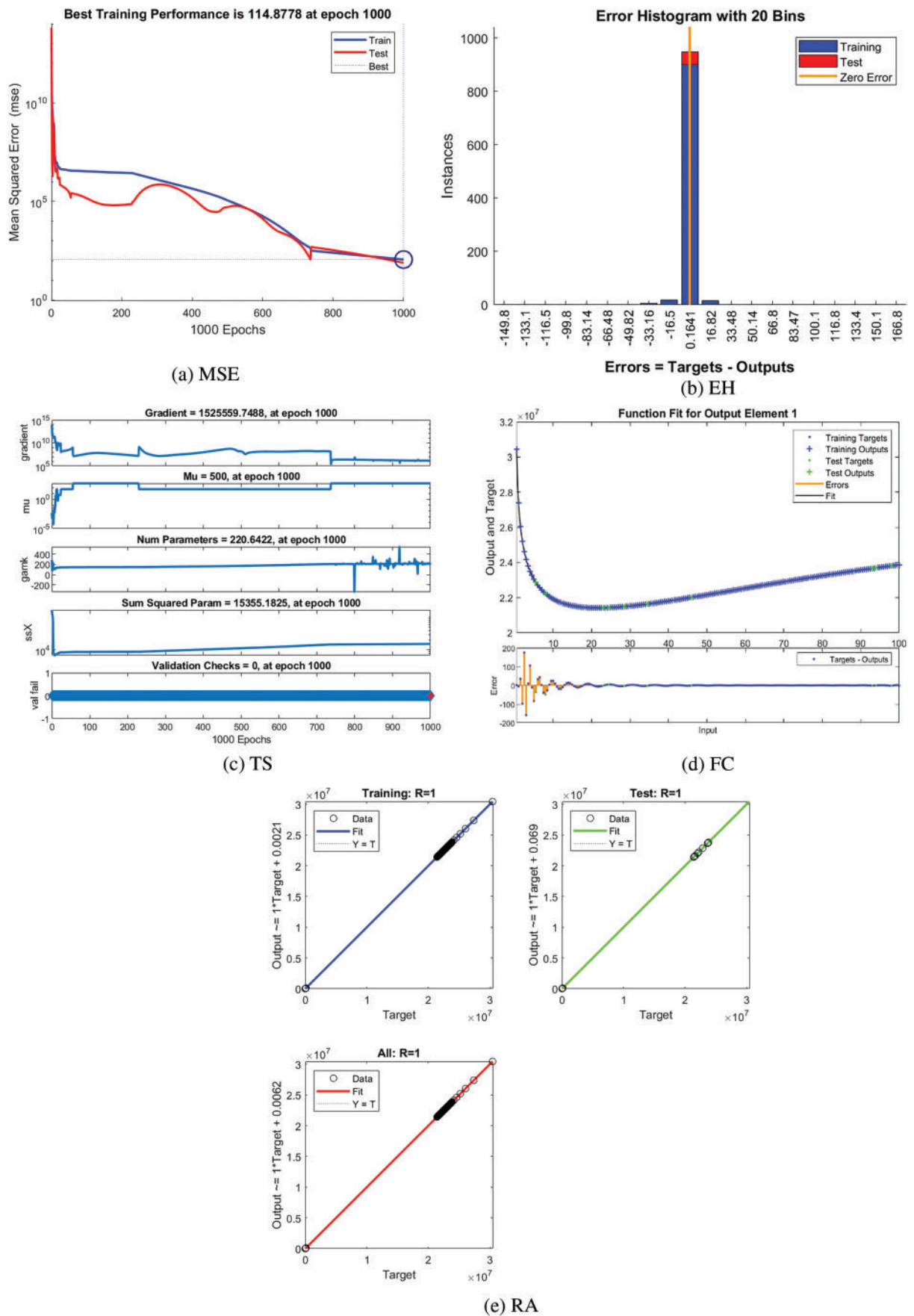


Figure 4: Graphical outputs based on BRA-NNs for scenario 2 case 3

Figs. 5 and 6 show a graphic representation of the FMTBV numerical results and absolute error (AE) for all situations, each with five cases. Despite the behavior of the TB virus model, we see Figs. 5 and 6a,c,e,g,i for  $\alpha = 0.80, 0.85, 0.90, 0.95, 1$ , respectively. We can see from Fig. 5a that the number of sensitive individuals grows as  $\alpha$  rises for scenario I, but in Fig. 6a the results fluctuated over time in scenario II. Fig. 5c,e,g,i shows that this tendency alters when  $\alpha$  increases, leading to a rapid increase in the population in the latent, infected, treated, and recovered classes. Similarly, in Fig. 6c,e,g, the results have a chaotic behavior whereas Fig. 6i by the increase of fractional order the recovery rate got increased. The simulation's outputs using BRA-NNs and the FOLotkaVolterra framework are essentially in line with the related AE. As can be observed, the AE for all cases is in the range of  $10^3 \rightarrow 10^{-5}$ . A visual representation of the AEs between actual (ground truth) values and anticipated values in a dataset is called an AE graph. It is frequently employed to assess the effectiveness of a regression model whose objective is to forecast continuous values. We can learn more about the model's performance by looking at the absolute error graph. It is preferable to have lower absolute errors and a more condensed distribution of vertical lines near 0, which show that the model's predictions are nearer to the actual values. On the other hand, a wide range of vertical lines with big absolute errors indicates that the model might need to be tweaked or improved.

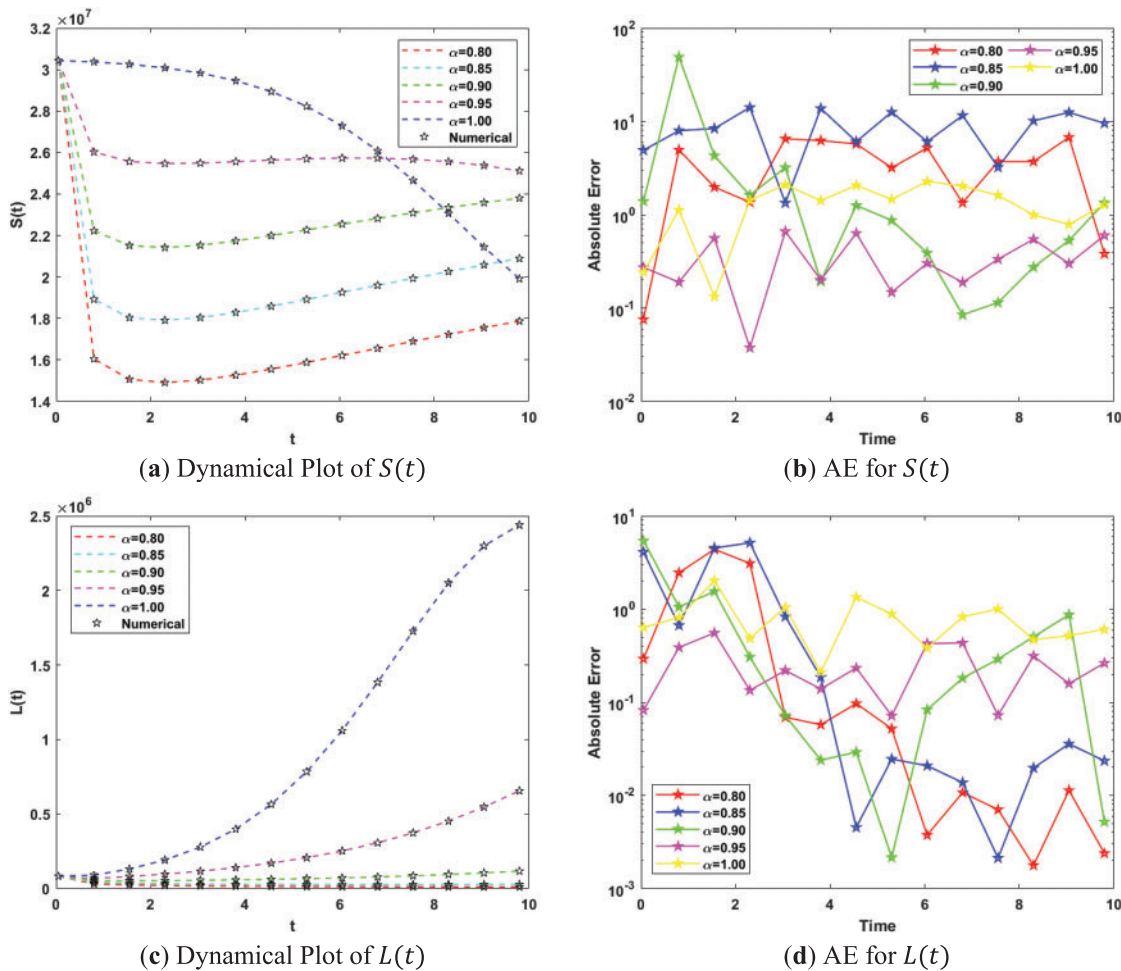
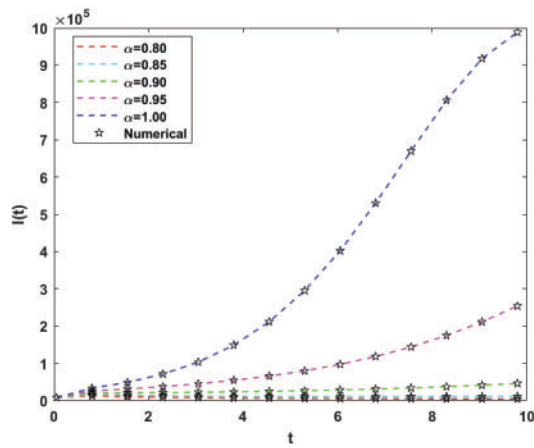
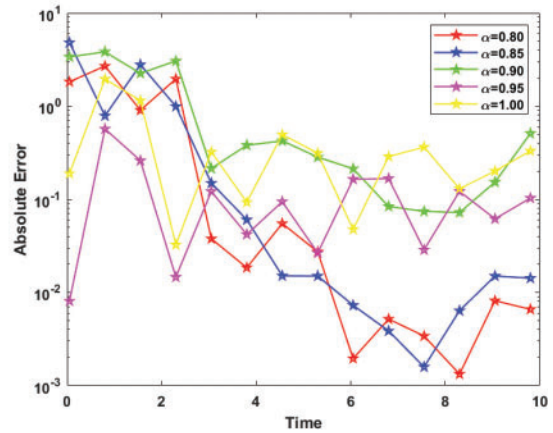


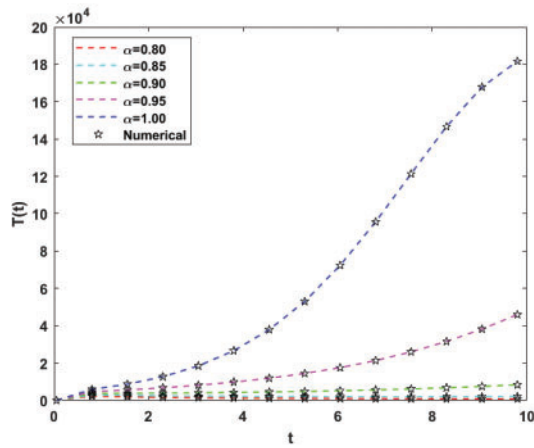
Figure 5: (Continued)



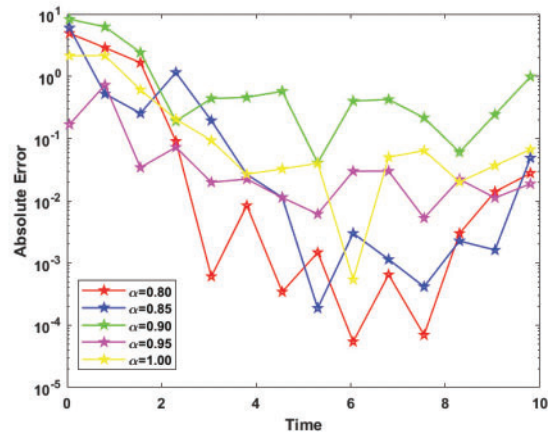
(e) Dynamical Plot of  $I(t)$



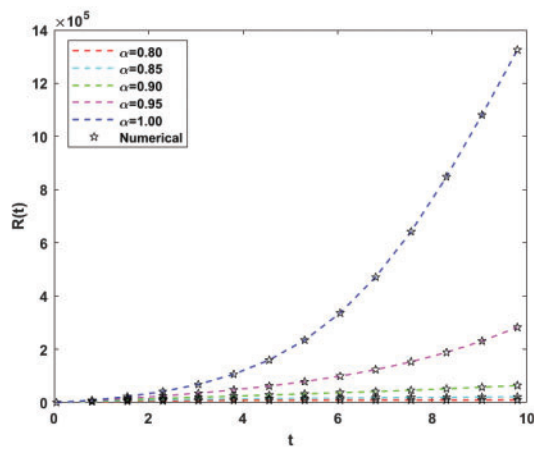
(f) AE for  $I(t)$



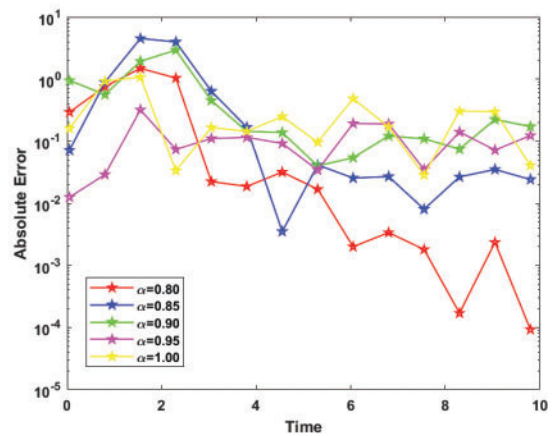
(g) Dynamical Plot of  $T(t)$



(h) AE for  $T(t)$

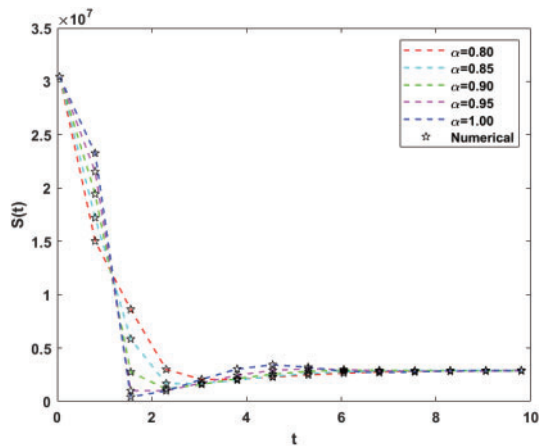


(i) Dynamical Plot of  $R(t)$

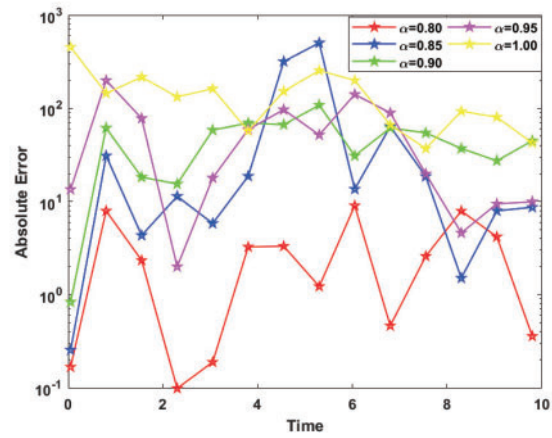


(j) AE for  $R(t)$

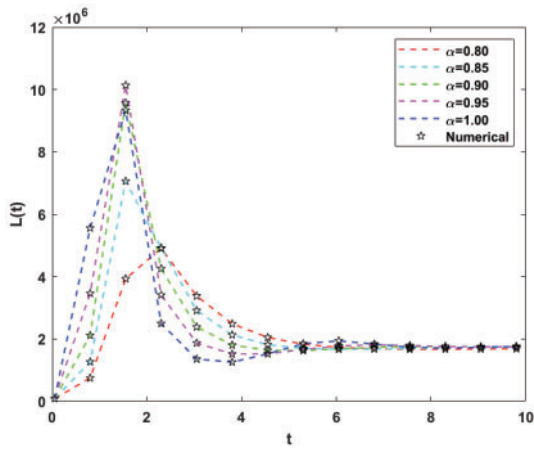
**Figure 5:** Dynamical and their corresponding absolute error plots of FMTBV for scenario-I



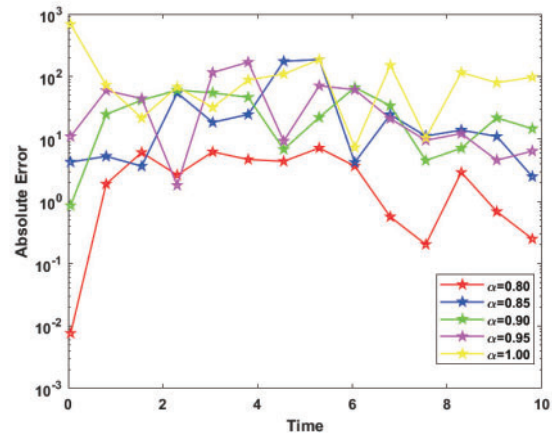
(a) Dynamical Plot of  $S(t)$



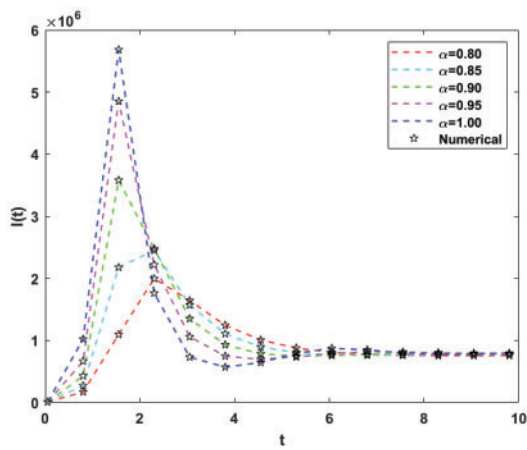
(b) AE for  $S(t)$



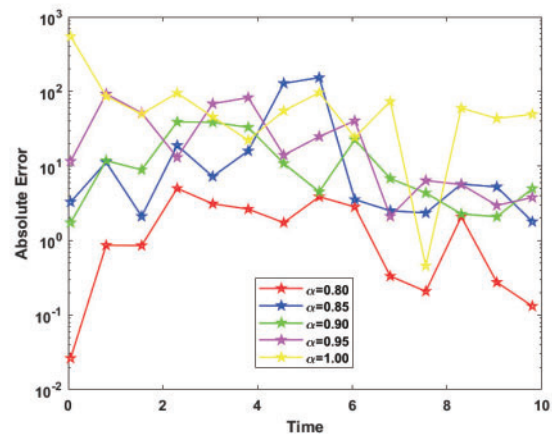
(c) Dynamical Plot of  $L(t)$



(d) AE for  $L(t)$



(e) Dynamical Plot of  $I(t)$



(f) AE for  $I(t)$

Figure 6: (Continued)

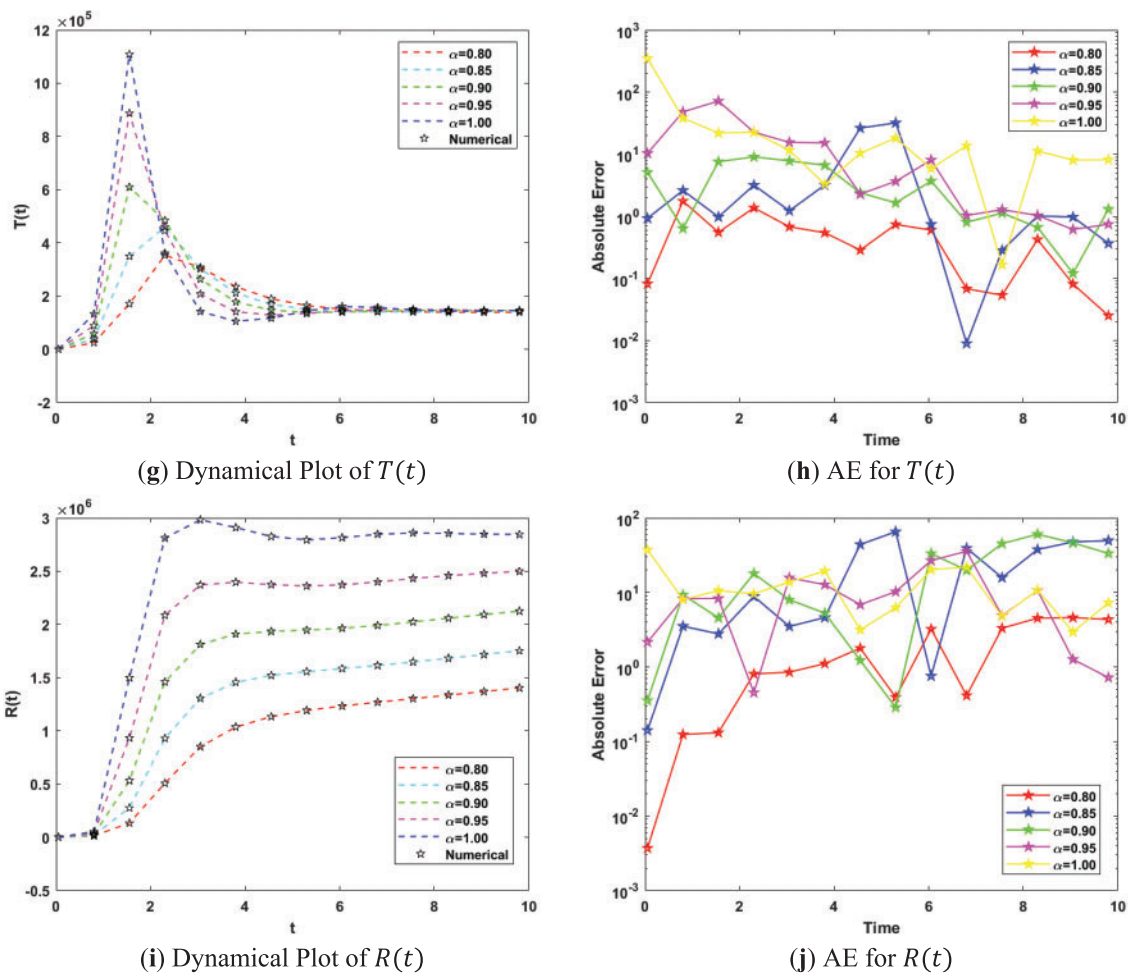


**Figure 6:** Dynamical and their corresponding absolute error plots of FMTBV for scenario-II

## 5 Conclusion

The TB-virus fractional model is discussed in this article. The purpose of this investigation is to supply a fractional order assessment using a mathematical structure with an emphasis on epidemic phenomena to deliver more reliable system efficiency. BRA-NNs are used to solve the FMTBV five-chamber design computationally. While the best under distinct conditions corresponded to different fractional orders, the orders of 0.80 and 0.95 were always the best in a comprehensive context. Such particular orders brought model precision together with computation efficiency, thus describing the subtle dynamics of the TB virus more effectively than other fractional values. The performance at 0.80 and 0.95 indicates that those orders are very well suited to the representation of the complexity inherent in the system, offering strong and reliable predictions across a variety of scenarios for simulations. The elements that follow are the main components of the mathematically calculated FMTBV findings:

- Using the suggested randomized computing paradigm offered by BRA-NNs, the FMTBV simulated solution has been effectively discovered. Modifications to the settings significantly alter how FMTBV functions.
- In scenario I, there is proper increase/decrease behavior of performance in all the  $S, L, I, T, R$  cases, but in scenario II, there is chaotic behavior with irregular fluctuations.

- For several circumstances, the AE magnitude ranged from  $10^3 \rightarrow 10^{-5}$ , suggesting accurate validation, testing, and training modeling. The great accuracy, as well as convergence of the developed technique, were proved by evaluations of the projected BRA-NNs findings along with the validated numerical answers provided by the FOLotkaVolterra scheme.
- Fitness graphs show how well the data was processed and how accurate the results were. Regression matrices, MSE learning curves, and histogram error visualizations show that the resultant BRA-NNs are efficient, reliable, and robust for full computations.

**Limitations:** The study's reliance on specific fractional orders (0.80 and 0.95) limits its generalizability to other epidemic models. While BRA-NNs improve computational efficiency, the lack of comparison with other numerical methods leaves uncertainty about its optimality. Additionally, chaotic behavior in Scenario II suggests sensitivity to parameter variations, requiring further stability analysis. The absence of validation with real-world TB data and exploration of alternative AI techniques also restricts the model's practical applicability.

In the future, the authors intend to implement AI solver based on transfer learning, physics-informing, and deep learning for epidemic systems.

**Acknowledgement:** The authors would like to thank the supported via funding from Prince Sattam bin Abdulaziz University project number (PSAU/2024/R/1445).

**Funding Statement:** This study is supported via funding from Prince Sattam bin Abdulaziz University project number (PSAU/2024/R/1445).

**Author Contributions:** The authors confirm contribution to the paper as follows: Study conception and design: Aqsa Zafar Abbasi, Ayesha Rafiq, Muhammad Shoaib; Analysis and interpretation of results: Muhammad Asif Zahoor Raja, Aqsa Zafar Abbasi, Kottakkaran Sooppy Nisar, Muhammad Shoaib; Draft manuscript preparation: Muhammad Asif Zahoor Raja, Aqsa Zafar Abbasi, Kottakkaran Sooppy Nisar, Ayesha Rafiq, Muhammad Shoaib; Validation: Muhammad Asif Zahoor Raja, Kottakkaran Sooppy Nisar; Visualization: Aqsa Zafar Abbasi, Ayesha Rafiq; Supervision: Muhammad Shoaib; Writing—review and editing: Aqsa Zafar Abbasi, Kottakkaran Sooppy Nisar, Muhammad Shoaib. All authors reviewed the results and approved the final version of the manuscript.

**Availability of Data and Materials:** All data generated or analyzed during this study are included in this published article.

**Ethics Approval:** Not applicable.

**Conflicts of Interest:** The authors declare no conflicts of interest to report regarding the present study.

## Nomenclature

FMTBV	Fractional model of TB virus
BRA-NNs	Bayesian regularized artificial neural network
GLs	Grunwald-Letnikov
$\Lambda, \sigma_2, \varepsilon, \xi, \gamma, \beta, \hat{u}, n, \sigma, \sigma_1$	Parameters of Model

Appendix A

**Table A1:** Simulations of BRA-NNs for FMTBV

Scenario	Case	Mean square error			Performance	Mu	Gradient	Epochs	Time
		Training	Validation	Testing					
S-I	I	18.63212E-00	0.0000E-00	9.12508E-00	<b>18.6</b>	500	1.31E-05	1000	18 s
	II	44.78196E-00	0.0000E-00	71.03747 E-00	44.8	50.0	4.04E-06	1000	20 s
	III	114.87782E-07	0.0000E-00	77.72245E-00	115	500	1.53E-06	1000	20 s
	IV	2.05271E-07	0.0000E-00	8.49377E-07	0.205	50.0	1.70E-05	1000	19 s
	V	1.22770E-08	0.0000E-00	1.73364E-00	1.23	500	1.51E-04	1000	20 s
S-II	I	13.50227 E-00	0.0000 E-00	27.47591 E-00	13.5	500	4.34E-05	1000	20 s
	II	268.60562 E-00	0.0000E-00	55.54794545 E-00	269	50.0	3.08E-05	1000	51 s
	III	1056.4347 E-00	0.0000E-00	2344.49074E-00	272	500	1.06E-03	1000	31 s
	IV	4285.52388 E-00	0.0000E-00	4290.01821 E-00	272	500	4.29E-03	1000	18 s
	V	13,745.539 51E-00	0.0000E-00	66,736.41415 E-00	271	500	1.37E-04	1000	19 s

**Table A2:** Data set for SI/CI

$t$	$S(t)$	$L(t)$	$I(t)$	$T(t)$	$R(t)$
0.5000	30432361	83000	8010	0	0
1	24,346,095.6146722	58,620.3027265495	13,572.8387959939	1321.73425474955	0
1.500	21,962,420.3133916	50,433.8953404672	14,321.5531956650	2115.32201164851	218.100054953600
2	20,562,799.5205937	45,905.6187283034	14,535.6364435187	2269.95153154265	521.680122218472
2.500	19,605,291.8580155	42,799.7755691519	14,515.5671051906	2396.51361394151	804.932183442074
3	18,894,979.8517505	40,508.8811059160	14,389.8114839113	2442.32361328388	1081.28047766835
3.500	18,340,942.2698431	38,699.1793176952	14,211.8276236869	2461.19141138679	1343.78706582586
4	17,893,841.0148119	37,210.9097206297	14,008.4492618553	2459.84410577268	1593.65030164086
4.500	17,524,085.4628792	35,947.1921384243	13,793.7007014898	2447.35491327219	1831.16690597844
5	17,212,615.2003427	34,848.6870040068	13,575.3659200906	2427.68922926422	2057.21900435744
5.500	16,946,476.2817403	33,876.0451344487	13,357.8433494139	2403.62345328350	2272.62930716556
6	16,716,488.9553668	33,002.2676846710	13,143.6425199593	2376.83205551880	2478.20626457393
6.500	16,515,926.1587317	32,208.0904148975	12,934.1725274372	2348.42563493267	2674.69032564751
7	16,339,720.6931027	31,479.3671168812	12,730.1877764349	2319.13540982477	2862.75447417244
7.500	16,183,966.9303223	30,805.4370023631	12,532.0462013630	2289.45457511229	3043.00451855872
8	16,045,595.3023561	30,178.0878156592	12,339.8638618541	2259.71772064073	3215.98479895394
8.500	15,922,152.6136571	29,590.8700504955	12,153.6093880388	2230.15317724321	3382.18441178416
9	15,811,649.5773861	29,038.6318271713	11,973.1627198020	2200.91655071119	3542.04354619576
9.500	15,712,452.4169834	28,517.1952073753	11,798.3520838391	2172.11308817213	3695.95933240270
10	15,623,204.1510636	28,023.1260686754	11,628.9774563045	2143.81275363681	3844.29108201207
10.50	15,542,766.3575930	27,553.5672665188	11,464.8254914289	2116.06057716582	3987.36488817814
11	15,470,175.3693274	27,106.1155577577	11,305.6789904355	2088.88385044563	4125.47762553564
11.50	15,404,608.8321127	26,678.7293641120	11,151.3228414057	2062.29719184342	4258.90041070771
12	15,345,359.8314468	26,269.6586515895	11,001.5476613689	2036.30614887515	4387.88159061831
12.50	15,291,816.6312495	25,877.3909215691	10,856.1519360232	2010.90978389786	4512.64932305946
13	15,243,446.6322635	25,500.6091099399	10,714.9431765374	1986.10254444522	4633.41380788913
13.50	15,199,783.5432517	25,138.1584046372	10,577.7384356593	1961.87562493633	4750.36922002569
14	15,160,417.0267314	24,789.0198244426	10,444.3644101367	1938.21796326830	4863.69538828562

(Continued)

**Table A2 (continued)**

$t$	$S(t)$	$L(t)$	$I(t)$	$T(t)$	$R(t)$
14.50	15,124,984.2708918	24,452.2889817761	10,314.6572807292	1915.11697305615	4973.55925758378
15	15,093,163.0755411	24,127.1588619268	10,188.4623908582	1892.55908300059	5080.11616626821
15.50	15,064,666.1388907	23,812.9057445421	10,065.6338313642	1870.53013457354	5183.51096541374
16	15,039,236.3047639	23,508.8776058557	9946.03397625082	1849.01567499936	5283.87900269800
16.50	15,016,642.5839382	23,214.4844960792	9829.53299902569	1828.00117245658	5381.34698994406
17	14,996,676.8040024	22,929.1905019598	9716.00838889330	1807.47217324760	5476.03377044659
17.50	14,979,150.7729670	22,652.5069910349	9605.34447902816	1787.41441551685	5568.05099971505
18	14,963,893.8654923	22,383.9868995079	9497.43199438649	1767.81391034736	5657.50375119169
18.50	14,950,750.9588385	22,123.2198755255	9392.16762329319	1748.65699832462	5744.49105676557
19	14,939,580.6598431	21,869.8281279732	9289.45361487812	1729.93038763832	5829.10639045013
19.50	14,930,253.7753584	21,623.4628606072	9189.19740300195	1711.62117829843	5911.43810237233
20	14,922,651.9873756	21,383.8011945325	9091.31125637893	1693.71687592787	5991.56980919702
20.50	14,916,666.7010455	21,150.5435002725	8995.71195401576	1676.20539776044	6069.58074624706
21	14,912,198.0393986	20,923.4110751011	8902.32048473278	1659.07507284418	6145.54608585124
21.50	14,909,153.9630593	20,702.1441128107	8811.06176934130	1642.31463797575	6219.53722583521
22	14,907,449.4968931	20,486.4999222935	8721.86440396664	1625.91323053050	6291.62205154749
22.50	14,907,006.0484794	20,276.2513587434	8634.66042299379	1609.86037907818	6361.86517436693
23	14,907,750.8057283	20,071.1854373000	8549.38508014599	1594.14599246364	6430.32814925847
23.50	14,909,616.2029452	19,871.1021038562	8465.97664626922	1578.76034787106	6497.06967361843
24	14,912,539.4462874	19,675.8131417666	8384.37622247488	1563.69407826573	6562.14576937230
24.50	14,916,462.0909203	19,485.1411964917	8304.52756738069	1548.93815951213	6625.60995004754
25	14,921,329.6633102	19,298.9189029428	8226.37693728110	1534.48389739323	6687.51337433777
25.50	14,927,091.3230402	19,116.9881025546	8149.87293816867	1520.32291469891	6747.90498749539
26	14,933,699.5593264	18,939.1991390024	8074.96638861561	1506.44713850742	6806.83165173507
26.50	14,941,109.9180848	18,765.4102230554	8001.61019260757	1492.84878774974	6864.33826669578
27	14,949,280.7559607	18,595.4868583893	7929.75922150005	1479.52036112037	6920.46788089204
27.50	14,958,173.0182129	18,429.3013212951	7859.37020434013	1466.45462537801	6975.26179498228
28	14,967,750.0377551	18,266.7321881715	7790.40162586310	1453.64460406380	7028.75965759321
28.50	14,977,977.3530000	18,107.6639054889	7722.81363153519	1441.08356665311	7080.99955436015
29	14,988,822.5424540	17,951.9863975993	7656.56793906950	1428.76501814765	7132.01809077450
29.50	15,000,255.0742635	17,799.5947083512	7591.62775589362	1416.68268910791	7181.85046936870
30	15,012,246.1691345	17,650.3886729699	7527.95770209396	1404.83052612094	7230.53056171529
30.50	15,024,768.6752375	17,504.2726170949	7465.52373840403	1393.20268269453	7278.09097566953
31	15,037,796.9538726	17,361.1550802380	7404.29309884241	1381.79351056627	7324.56311824254
31.50	15,051,306.7748147	17,220.9485612479	7344.23422764086	1370.59755141426	7369.97725445512
32	15,065,275.2203807	17,083.5692836438	7285.31672013457	1359.60952895461	7414.36256248884
32.50	15,079,680.5973683	16,948.9369789262	7227.51126731498	1348.82434141052	7457.74718542158
33	15,094,502.3561136	16,816.9746861801	7170.78960377177	1338.23705433709	7500.15827980820
33.50	15,109,721.0159925	16,687.6085664739	7115.12445877368	1327.84289378600	7541.62206134359
34	15,125,318.0967681	16,560.7677307158	7060.48951025933	1317.63723979445	7582.16384782379
34.50	15,141,276.0552466	16,436.3840797741	7006.85934152837	1307.61562018265	7621.80809960246
35	15,157,578.2267626	16,314.3921557886	6954.20940044071	1297.77370464510	7660.57845772241
35.50	15,174,208.7710624	16,194.7290037152	6902.51596094755	1288.10729912084	7698.49777988676
36	15,191,152.6222002	16,077.3340422364	6851.75608679227	1278.61234042873	7735.58817442050
36.50	15,208,395.4420973	15,962.1489432632	6801.90759723224	1269.28489115428	7771.87103236060
37	15,225,923.5774530	15,849.1175193233	6752.94903464483	1260.12113477505	7807.36705780156
37.50	15,243,724.0197233	15,738.1856182039	6704.85963389114	1251.11737101245	7842.09629661304
38	15,261,784.3679117	15,629.3010242730	6657.61929332169	1242.27001139816	7876.07816363705
38.50	15,280,092.7939425	15,522.4133659603	6611.20854731641	1233.57557504395	7909.33146846345
39	15,298,638.0104046	15,417.4740289226	6565.60854026019	1225.03068460456	7941.87443987526
39.50	15,317,409.2404789	15,314.4360744675	6520.80100186236	1216.63206242348	7973.72474904787
40	15,336,396.1898733	15,213.2541628404	6476.76822373544	1208.37652685221	8004.89953158026
40.50	15,355,589.0206116	15,113.8844810203	6433.49303715488	1200.26098873399	8035.41540843030

(Continued)

Table A2 (continued)

$t$	$S(t)$	$L(t)$	$I(t)$	$T(t)$	$R(t)$
41	15,374,978.3265305	15,016.2846746974	6390.95879192703	1192.28244804368	8065.28850582088
41.50	15,394,555.1103562	14,920.4137841351	6349.14933629805	1184.43799067558	8094.53447417907
42	15,414,310.7622410	14,826.2321836426	6308.04899784115	1176.72478537181	8123.16850616558
42.50	15,434,237.0396507	14,733.7015244090	6267.64256526418	1169.14008078397	8151.20535384820
43	15,454,326.0485041	14,642.7846804691	6227.91527108339	1161.68120266145	8178.65934506885
43.50	15,474,570.2254729	14,553.4456975890	6188.85277511323	1154.34555115993	8205.54439905047
44	15,494,962.3213593	14,465.6497448785	6150.44114872519	1147.13059826412	8231.87404128703
44.50	15,515,495.3854731	14,379.3630689511	6112.66685983222	1140.03388531901	8257.66141775670
45	15,536,162.7509398	14,294.5529504663	6075.51675855785	1133.05302066431	8282.91930849590
45.50	15,556,958.0208739	14,211.1876629026	6038.97806355208	1126.18567736698	8307.66014056903
46	15,577,875.0553570	14,129.2364334204	6003.03834891849	1119.42959104709	8331.89600046694
46.50	15,598,907.9591684	14,048.6694056844	5967.68553171941	1112.78255779247	8355.63864596464
47	15,620,051.0702147	13,969.4576045251	5932.90786002802	1106.24243215787	8378.89951746684
47.50	15,641,298.9486132	13,891.5729023278	5898.69390149827	1099.80712524466	8401.68974886855
48	15,662,646.3663861	13,814.9879870461	5865.03253242554	1093.47460285710	8424.02017795556
48.50	15,684,088.2977250	13,739.6763317421	5831.91292727216	1087.24288373173	8445.90135636880
49	15,705,619.9097887	13,665.6121655655	5799.32454863411	1081.11003783635	8467.34355915457
49.50	15,727,236.5540010	13,592.7704460873	5767.25713762628	1075.07418473545	8488.35679392151
50	15,748,933.7578162	13,521.1268329114	5735.70070466503	1069.13349201889	8508.95080962426
50.50	15,770,707.2169222	13,450.6576624911	5704.64552062833	1063.28617379107	8529.13510499169
51	15,792,552.7878561	13,381.3399240836	5674.08210837464	1057.53048921778	8548.91893661771
51.50	15,814,466.4810043	13,313.1512367797	5644.00123460299	1051.86474112809	8568.31132673057
52	15,836,444.4539659	13,246.0698275498	5614.39390203768	1046.28727466886	8587.32107065628
52.50	15,858,483.0052558	13,180.0745102504	5585.25134192187	1040.79647600959	8605.95674399072
53	15,880,578.5683284	13,115.1446655423	5556.56500680546	1035.39077109519	8624.22670949407
53.50	15,902,727.7059015	13,051.2602216685	5528.32656361318	1030.06862444481	8642.13912372064
54	15,924,927.1045645	12,988.4016360504	5500.52788697996	1024.82853799449	8659.70194339634
54.50	15,947,173.5696530	12,926.5498776578	5473.16105284103	1019.66904998200	8676.92293155516
55	15,969,464.0203746	12,865.6864101134	5446.21833226499	1014.58873387176	8693.80966344601
55.50	15,991,795.4851717	12,805.7931754948	5419.69218551894	1009.58619731836	8710.36953221993
56	16,014,165.0973088	12,746.8525787994	5393.57525635504	1004.66008116696	8726.60975440760
56.50	16,036,570.0906695	12,688.8474730383	5367.86036650862	999.809058489018	8742.53737519661
57	16,059,007.7957537	12,631.7611449283	5342.54051039839	995.031833651888	8758.15927351695
57.50	16,081,475.6358628	12,575.5773011540	5317.60885001993	990.327141420844	8773.48216694347
58	16,103,971.1234624	12,520.2800551712	5293.05871002395	985.693746092262	8788.51261642283
58.50	16,126,491.8567140	12,465.8539145261	5268.88357297130	981.130440656637	8803.25703083289
59	16,149,035.5161654	12,412.2837686664	5245.07707475718	976.636045990232	8817.72167138130
59.50	16,171,599.8615915	12,359.5548772199	5221.63300019727	972.209410074210	8831.91265585022
60	16,194,182.7289785	12,307.6528587205	5198.54527876902	967.849407240144	8845.83596269377
60.50	16,216,782.0276431	12,256.5636797599	5175.80798050147	963.554937440861	8859.49743499403
61	16,239,395.7374790	12,206.2736445456	5153.41531200746	959.324925545609	8872.90278428164
61.50	16,262,021.9063261	12,156.7693848473	5131.36161265247	955.158320658592	8886.05759422652
62	16,284,658.6474539	12,108.0378503138	5109.64135085423	951.054095459977	8898.96732420392
62.50	16,307,304.1371552	12,060.0662991444	5088.24912050794	947.011245568474	8911.63731274078
63	16,329,956.6124430	12,012.8422890985	5067.17963753210	943.028788924680	8924.07278084742
63.50	16,352,614.3688461	11,966.3536688289	5046.42773652993	939.105765194389	8936.27883523889
64	16,375,275.7582987	11,920.5885695259	5025.98836756180	935.241235191098	8948.26047145034
64.50	16,397,939.1871189	11,875.5353968558	5005.85659302445	931.434280316990	8960.02257685078
65	16,420,603.1140719	11,831.1828231855	4986.02758463266	927.684002021699	8971.56993355891
65.50	16,443,266.0485139	11,787.5197800768	4966.49662049936	923.989521278198	8982.90722126506
66	16,465,926.5486128	11,744.5354510426	4947.25908231050	920.349978075166	8994.03901996252
66.50	16,488,583.2196413	11,702.2192645514	4928.31045259084	916.764530925228	9004.96981259215
67	16,511,234.7123404	11,660.5608872722	4909.64631205748	913.232356388492	9015.70398760311

(Continued)

**Table A2 (continued)**

$t$	$S(t)$	$L(t)$	$I(t)$	$T(t)$	$R(t)$
67.50	16,533,879.7213486	11,619.5502175474	4891.26233705747	909.752648610813	9026.24584143318
68	16,556,516.9836943	11,579.1773790872	4873.15429708654	906.324618876278	9036.59958091148
68.50	16,579,145.2773486	11,539.4327148741	4855.31805238595	902.947495173352	9046.76932558664
69	16,601,763.4198353	11,500.3067812706	4837.74955161435	899.620521774252	9056.75910998297
69.50	16,624,370.2668955	11,461.7903423216	4820.44482959207	896.342958827036	9066.57288578751
70	16,646,964.7112052	11,423.8743642434	4803.40000511513	893.114081959966	9076.21452397013
70.50	16,669,545.6811417	11,386.5500100927	4786.61127883633	889.933181897737	9085.68781683959
71	16,692,112.1395986	11,349.8086346085	4770.07493121120	886.799564089122	9094.99648003733
71.50	16,714,663.0828457	11,313.6417792189	4753.78732050625	883.712548345658	9104.14415447162
72	16,737,197.5394327	11,278.0411672091	4737.74488086744	880.671468490985	9113.13440819400
72.50	16,759,714.5691343	11,242.9986990414	4721.94412044661	877.675672020475	9121.97073822003
73	16,782,213.2619355	11,208.5064478241	4706.38161958402	874.724519770779	9130.65657229645
73.50	16,804,692.7370537	11,174.5566549220	4691.05402904474	871.817385599005	9139.19527061650
74	16,827,152.1419988	11,141.1417257037	4675.95806830731	868.953656071114	9147.59012748511
74.50	16,849,590.6516668	11,108.2542254215	4661.09052390263	866.132730159339	9155.84437293602
75	16,872,007.4674674	11,075.8868752170	4646.44824780145	863.354018948201	9163.96117430200
75.50	16,894,401.8164831	11,044.0325482502	4632.02815584878	860.616945348950	9171.94363774026
76	16,916,772.9506592	11,012.6842659459	4617.82722624362	857.920943822055	9179.79480971420
76.50	16,939,120.1460229	10,981.8351943537	4603.84249806243	855.265460107548	9187.51767843311
77	16,961,442.7019301	10,951.4786406177	4590.07106982496	852.649950962932	9195.11517525130
77.50	16,983,739.9403400	10,921.6080495519	4576.51009810093	850.073883908398	9202.59017602785
78	17,006,011.2051141	10,892.2170003174	4563.15679615616	847.536736979158	9209.94550244839
78.50	17,028,255.8613418	10,863.2992031978	4550.00843263708	845.037998484588	9217.18392331019
79	17,050,473.2946874	10,834.8484964697	4537.06233029197	842.577166774060	9224.30815577165
79.50	17,072,662.9107619	10,806.8588433651	4524.31586472812	840.153750009154	9231.32086656745
80	17,094,824.1345156	10,779.3243291210	4511.76646320346	837.767265942112	9238.22467319041
80.50	17,116,956.4096518	10,752.2391581161	4499.41160345166	835.417241700307	9245.02214504119
81	17,139,059.1980608	10,725.5976510885	4487.24881253958	833.103213576557	9251.71580454682
81.50	17,161,131.9792729	10,699.3942424341	4475.27566575611	830.824726825059	9258.30812824901
82	17,183,174.2499308	10,673.6234775811	4463.48978553128	828.581335462840	9264.80154786335
82.50	17,205,185.5232784	10,648.2800104399	4451.88884038468	826.372602076470	9271.19845131018
83	17,227,165.3286685	10,623.3586009242	4440.47054390251	824.198097633937	9277.50118371803
83.50	17,249,113.2110856	10,598.8541125416	4429.23265374192	822.057401301511	9283.71204840059
84	17,271,028.7306850	10,574.7615100522	4418.17297066224	819.950100265407	9289.83330780799
84.50	17,292,911.4623477	10,551.0758571913	4407.28933758189	817.875789558167	9295.86718445294
85	17,314,760.9952492	10,527.7923144561	4396.57963866051	815.834071889548	9301.81586181307
85.50	17,336,576.9324424	10,504.9061369519	4386.04179840519	813.824557481844	9307.68148520956
86	17,358,358.8904553	10,482.4126722987	4375.67378080034	811.846863909453	9313.46616266330
86.50	17,380,106.4988999	10,460.3073585939	4365.47358846037	809.900615942600	9319.17196572887
87	17,401,819.4000954	10,438.5857224304	4355.43926180441	807.985445395082	9324.80093030725
87.50	17,423,497.2487024	10,417.2433769687	4345.56887825259	806.100990975904	9330.35505743788
88	17,445,139.7113695	10,396.2760200597	4335.86055144301	804.246898144706	9335.83631407060
88.50	17,466,746.4663906	10,375.6794324190	4326.31243046899	802.422818970862	9341.24663381804
89	17,488,317.2033733	10,355.4494758484	4316.92269913583	800.628411996156	9346.58791768927
89.50	17,509,851.6229180	10,335.5820915061	4307.68957523661	798.863342100896	9351.86203480495
90	17,531,349.4363066	10,316.0732982208	4298.61130984641	797.127280373423	9357.07082309475
90.50	17,552,810.3652013	10,296.9191908515	4289.68618663443	795.419903982857	9362.21608997748
91	17,574,234.1413523	10,278.1159386892	4280.91252119348	793.740896055030	9367.29961302444
91.50	17,595,620.5063152	10,259.6597839008	4272.28866038632	792.089945551497	9372.32314060646
92	17,616,969.2111766	10,241.5470400129	4263.81298170847	790.466747151536	9377.28839252515
92.50	17,638,280.0162881	10,223.7740904351	4255.48389266673	788.871001137070	9382.19706062874
93	17,659,552.6910091	10,206.3373870207	4247.29983017337	787.302413280383	9387.05080941297
93.50	17,680,787.0134562	10,189.2334486648	4239.25925995515	785.760694734624	9391.85127660758

(Continued)

Table A2 (continued)

$t$	$S(t)$	$L(t)$	$I(t)$	$T(t)$	$R(t)$
94	17,701,982.7702614	10,172.4588599378	4231.36067597707	784.245561926945	9396.60007374869
94.50	17,723,139.7563370	10,156.0102697535	4223.60259988011	782.756736454262	9401.29878673728
95	17,744,257.7746474	10,139.8843900712	4215.98358043292	781.293944981511	9405.94897638471
95.50	17,765,336.6359883	10,124.0779946300	4208.50219299673	779.856919142383	9410.55217894501
96	17,786,376.1587717	10,108.5879177148	4201.15703900339	778.445395442428	9415.10990663471
96.50	17,807,376.1688181	10,093.4110529541	4193.94674544592	777.059115164487	9419.62364814051
97	17,828,336.4991540	10,078.5443521460	4186.86996438153	775.697824276371	9424.09486911495
97.50	17,849,256.9898162	10,063.9848241149	4179.92537244638	774.361273340751	9428.52501266055
98	17,870,137.4876611	10,049.7295335952	4173.11167038213	773.049217427167	9432.91549980275
98.50	17,890,977.8461800	10,035.7756001433	4166.42758257370	771.761416026123	9437.26772995189
99	17,911,777.9253193	10,022.1201970755	4159.87185659809	770.497632965205	9441.58308135458
99.50	17,932,537.5913068	10,008.7605504325	4153.44326278385	769.257636327173	9445.86291153464
100	17,953,256.7164819	9995.69393796847	4147.14059378095	768.041198369941	9450.10855772411

## References

1. Ai JW, Ruan QL, Liu QH, Zhang WH. Updates on the risk factors for latent tuberculosis reactivation and their managements. *Emerg Microbes Infect.* 2016;5(2):e10. doi:10.1038/emi.2016.10.
2. Chakaya J, Khan M, Ntoumi F, Akillu E, Fatima R, Mwaba P, et al. Global tuberculosis report 2020-reflections on the global TB burden, treatment and prevention efforts. *Int J Infect Dis.* 2021;113(Suppl 1):S7–12. doi:10.1016/j.ijid.2021.02.107.
3. Alade TO, Alnegga M, Olaniyi S, Abidemi A. Mathematical modelling of within-host Chikungunya virus dynamics with adaptive immune response. *Model Earth Syst Environ.* 2023;9(4):3837–49. doi:10.1007/s40808-023-01737-y.
4. Feng Z, Castillo-Chavez C, Capurro AF. A model for tuberculosis with exogenous reinfection. *Theor Popul Biol.* 2000;57(3):235–47. doi:10.1006/tpbi.2000.1451.
5. Huo HF, Zou MX. Modelling effects of treatment at home on tuberculosis transmission dynamics. *Appl Math Model.* 2016;40(21–22):9474–84. doi:10.1016/j.apm.2016.06.029.
6. Sweilam NH, Al-Mekhlafi SM, Baleanu D. Optimal control for a fractional tuberculosis infection model including the impact of diabetes and resistant strains. *J Adv Res.* 2019;17:125–37. doi:10.1016/j.jare.2019.01.007.
7. Altaf Khan M, Khan K, Safi MA, DarAssi MH. A discrete model of TB dynamics in khyber pakhtunkhwa-Pakistan. *Comput Model Eng Sci.* 2020;123(2):777–95. doi:10.32604/cmesci.2020.08208.
8. Owolabi KM, Pindza E. A nonlinear epidemic model for tuberculosis with Caputo operator and fixed point theory. *Healthc Anal.* 2022;2(3):100111. doi:10.1016/j.health.2022.100111.
9. Avazzadeh Z, Hassani H, Agarwal P, Mehrabi S, Ebadi MJ, Dahaghin MS. An optimization method for studying fractional-order tuberculosis disease model via generalized Laguerre polynomials. *Soft Comput.* 2023;27(14):9519–31. doi:10.1007/s00500-023-08086-z.
10. Ullah I, Ahmad S, Arfan M, De la Sen M. Investigation of fractional order dynamics of tuberculosis under caputo operator. *Fractal Fract.* 2023;7(4):300. doi:10.3390/fractalfract7040300.
11. Farman M, Mehmood Malik S, Akgül A, Ghaffari AS, Salamat N. Analysis and dynamical transmission of tuberculosis model with treatment effect by using fractional operator. *Int J Model Simul.* 2024;2024(2):1–15. doi:10.1080/02286203.2024.2392222.
12. Khan A, Shah K, Abdeljawad T, Amacha I. Fractal fractional model for tuberculosis: existence and numerical solutions. *Sci Rep.* 2024;14(1):12211. doi:10.1038/s41598-024-62386-4.
13. Ahmad Naik P, Yeolekar BM, Qureshi S, Yeolekar M, Madzvamuse A. Modeling and analysis of the fractional-order epidemic model to investigate mutual influence in HIV/HCV co-infection. *Nonlinear Dyn.* 2024;112(13):11679–710. doi:10.1007/s11071-024-09653-1.

14. Ahmad Naik P, Yeolekar BM, Qureshi S, Manhas N, Ghoreishi M, Yeolekar M, et al. Global analysis of a fractional-order hepatitis B virus model under immune response in the presence of cytokines. *Adv Theory Simul.* 2024;7(12):2400726. doi:10.1002/adts.202400726.
15. Anwar N, Ahmad I, Raja MAZ, Naz S, Shoaib M, Kiani AK. Artificial intelligence knacks-based stochastic paradigm to study the dynamics of plant virus propagation model with impact of seasonality and delays. *Eur Phys J Plus.* 2022;137(1):144. doi:10.1140/epjp/s13360-021-02248-4.
16. Raja MAZ, Naz H, Shoaib M, Mehmood A. Design of backpropagated neurocomputing paradigm for Stuxnet virus dynamics in control infrastructure. *Neural Comput Appl.* 2022;34(7):5771–90. doi:10.1007/s00521-021-06721-0.